

Article

Synthesis and Characterization of Charge Transfer Salts Based on $[M(\text{dcdmp})_2]$ ($M = \text{Au}, \text{Cu}$ and Ni) with TTF Type Donors

Rafaela A. L. Silva, Isabel C. Santos, Sandra Rabaça, Elsa B. Lopes, Vasco Gama, Manuel Almeida  and Dulce Belo * 

^C2TN, Centro de Ciências e Tecnologias Nucleares, Instituto Superior Técnico, Universidade de Lisboa, E.N. 10 ao km 139.7, 2695-066 Bobadela LRS, Portugal; rafaela@ctn.tecnico.ulisboa.pt (R.A.L.S.); icsantos@ctn.tecnico.ulisboa.pt (I.C.S.); sandrar@ctn.tecnico.ulisboa.pt (S.R.); eblopes@ctn.tecnico.ulisboa.pt (E.B.L.); vascog@ctn.tecnico.ulisboa.pt (V.G.); malmeida@ctn.tecnico.ulisboa.pt (M.A.)

* Correspondence: dbelo@ctn.tecnico.ulisboa.pt; Tel.: +351-21-955-6203

Received: 6 March 2018; Accepted: 17 March 2018; Published: 20 March 2018

Abstract: The charge transfer salts α -DT-TTF[Au(dcdmp)₂] (**1**), BET-TTF[Au(dcdmp)₂] (**2M** and **2T**), α -DT-TTF[Cu(dcdmp)₂] (**3**), ET[Cu(dcdmp)₂] (**4**), (BET-TTF)₂[Cu(dcdmp)₂] (**5**), (ET)₂[Ni(dcdmp)₂] (**6**), and α -mtdt[Cu(dcdmp)₂] (**7**) were obtained by electrocrystallization of different electron donor molecules derived from TTF (α -DT-TTF = alpha-dithiophene-tetrathiafulvalene; BET-TTF = (bis(ethylenethio)tetrathiafulvalene; ET = bis(ethylenedithio)-tetrathiafulvalene; α -mtdt = alpha-methylthiophenetetrathiafulvalene) in the presence of transition metal complex $[M(\text{dcdmp})_2]$ ($M = \text{Au}$ (III), Cu (III) and Ni (II)) (dcdmp = 2,3-dicyano-5,6-dimercaptopyrazine). Compounds **1** and **2** (**2M** and **2T**) have a similar packing pattern composed of mixed stacks of alternating donor-acceptor molecules. For (BET-TTF)[Au(dcdmp)₂] two different crystal structures (**2M** and **2T**) were obtained indicating polymorphism. Compounds **3** and **4** are isostructural being composed of zigzag chains of alternating donor and acceptor molecules. The salts with a 2:1 stoichiometry, (BET-TTF)₂[Cu(dcdmp)₂] (**5**), and (ET)₂[Ni(dcdmp)₂] (**6**) present the donor molecules fully oxidized and $[M(\text{dcdmp})_2]$ ($M = \text{Ni}$ and Cu) in a dianionic state. The salt of the dissymmetric donor α -mtdt with $[Cu(\text{dcdmp})_2]$, α -mtdt[Cu(dcdmp)₂] (**7**) has a crystal structure composed of segregated donor stacks that are positioned in a head-to-head fashion and alternate with the anion stacks. All charge transfer salts (**1–7**) are modest semiconductors with conductivities in the range 10^{-1} – 10^{-5} S/cm, with the highest values obtained in α -DT-TTF salts, compounds **1** and **3**.

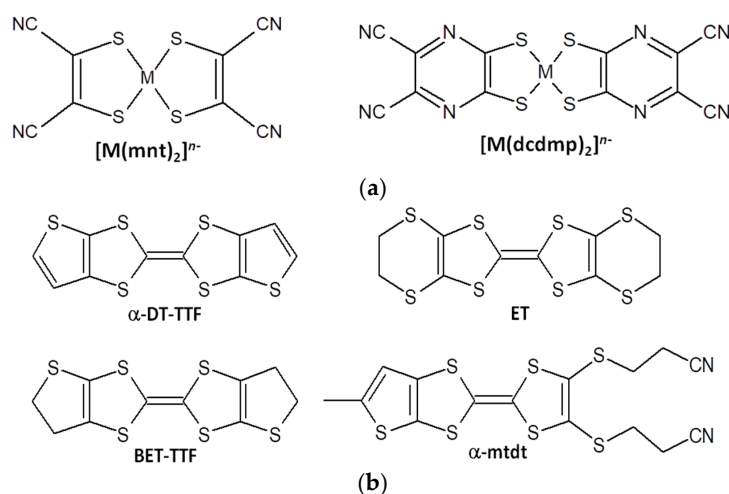
Keywords: charge transfer salts; TTF donors; dimercaptopyrazine bisdithiolate complexes; crystal engineering

1. Introduction

After about 50 years of intensive studies, transition metal bisdithiolene complexes still continue to be actively explored as building blocks for molecular conducting and magnetic materials due to their interesting and unique structural and electronic properties [1]. Some attractive features of these types of complexes are the diversity of coordination geometries that metal centres can adopt, as well as, depending on the transition metal or the oxidation state, the accessibility to several oxidation states and different magnetic moments [2]. The square planar coordination geometry and the delocalised π -nature of the ligands favour, in the solid state, the formation of extended networks of π - π interactions, which can give rise to interesting properties such as ferromagnetism [3], spin-ladder behaviour [4,5], and metallic [6,7], or even superconducting, properties [8,9].

Extended dithiolene π -ligands containing N atoms are significantly less explored when compared to sulphur rich ligands, which have been favoured to build intermolecular S \cdots S contacts with improved dimensionality in the solid state [10]. However, the N atoms in dithiolene ligands are now known to act as an extra coordinating site that can provide an additional degree of freedom in the crystal engineering of these solids [11].

$[M(\text{dcdmp})_2]$ complexes based on extended dithiolene π -ligand-containing N atoms (Scheme 1a) are, in this context, attractive anions. The dcdmp ligand as an extended π -system is expected to be able to increase the electronic delocalization, and the pyrazine nitrogen atoms can lead to an increase of intermolecular interactions [11–14] when compared with complexes based on other ligands such as mnt (mnt = maleonitriedithiolate) (Scheme 1a). The Au, Ni, and Cu complexes were previously combined with TTF-type donors, resulting in salts of different stoichiometries, including $(\text{DT-TTF})_2[\text{Cu}(\text{dcdmp})_2]$ (DT-TTF = dithiophene-tetrathiafulvalene) with a ladder-like structure [15,16]. In order to further explore $[M(\text{dcdmp})_2]$ anions as possible building blocks for molecular materials, these complexes with $M = \text{Au}, \text{Cu},$ and Ni were combined with different donors related to DT-TTF; the aromatic α -DT-TTF, the non-aromatic BET-TTF, the disymmetric thiophenic derivative α -mtdt, and the well-known ET donor (Scheme 1b). The electrical transport properties of salts will critically depend on the relative oxidation state of the molecular building blocks and their capability to establish extended networks of regular interactions. Salts in 1:1 stoichiometry, with full charge transfer between donor and acceptor, lead to half-filled bands, which, in molecular systems with narrow bands, will invariably behave as Mott insulators. Therefore, partial oxidation of the molecular building blocks in a regular network of strong interactions is usually a condition for high electrical conductivity. However, in spite of recent progresses in crystal engineering, both the stoichiometry and crystal structure of molecular salts remain largely unpredictable [1,4].



Scheme 1. Molecular diagram of transition metal bisdithiolene complexes (a) and of TTF type donors (b).

2. Materials and Methods

2.1. General Information

The donors BET-TTF [17], α -DT-TTF [18], and α -mtdt [19] were prepared as previously described, while ET was commercially obtained (Sigma-Aldrich, Darmstadt, Germany) and used without further purification. $(n\text{-Bu}_4\text{N})[M(\text{dcdmp})_2]$ ($M = \text{Au}$ and Cu) [20,21] and $(n\text{-Bu}_4\text{N})_2[\text{Ni}(\text{dcdmp})_2]$ [22] were prepared and purified by recrystallization following previously described procedures. Electrocrystallization was carried out in H-shaped two-compartment cells separated by frit glass with Pt electrodes and under galvanostatic conditions. All solvents were purified using standard procedures and freshly distilled immediately before its use [23].

2.2. Synthesis

α -DT-TTF[Au(dcdmp)₂] (1). Crystals were obtained by electrocrystallization from a dichloromethane solution of BET-TTF and (*n*-Bu₄N)[Au(dcdmp)₂][−], both 1 × 10^{−3} M. The system was sealed under nitrogen and after 10 days by applying a current density of 1.0 μA·cm^{−2}; brown plate crystals were collected and washed with dichloromethane.

BET-TTF[Au(dcdmp)₂] (2M and 2T). Crystals were obtained by electrocrystallization from a dichloromethane solution of BET-TTF and (*n*-Bu₄N)[Au(dcdmp)₂][−], following the same procedure as described for compound 1. Brown plate crystals were collected after 9 days by applying a current density of 1.0 μA·cm^{−2}.

α -DT-TTF[Cu(dcdmp)₂] (3). Crystals were obtained by electrocrystallization from a dichloromethane solution of BET-TTF and (*n*-Bu₄N)[Cu(dcdmp)₂][−], following the same procedure as described for compound 1. Brown plate crystals were collected after 10 days by applying a current density of 1.0 μA·cm^{−2}.

ET[Cu(dcdmp)₂] (4). Crystals were obtained by electrocrystallization from an acetonitrile solution of the ET donor (2 × 10^{−2} mmol) and copper acceptor salt (5 × 10^{−2} mmol). The system was sealed under nitrogen and after 18 days, with a current density of 1.0 μA·cm^{−2}; black prism shape crystals were collected and washed with acetonitrile.

(BET-TTF)₂[Cu(dcdmp)₂] (5). Crystals were obtained by electrocrystallization of BET-TTF donor and tetrabutylammonium salt of [Cu(dcdmp)₂][−] as electrolyte, following the same procedure as described for compound 1. Brown plate crystals were collected after 12 days by applying a current density of 1.0 μA·cm^{−2}.

(ET)₂[Ni(dcdmp)₂] (6). Crystals were obtained by electrocrystallization from a dichloromethane solution of the donor and nickel acceptor salt in approximately stoichiometric amounts. The system was sealed under nitrogen and after 18 days, with a current density of 0.5 μA·cm^{−2}; brown plate shape crystals were collected and washed with dichloromethane.

α -mtdt[Cu(dcdmp)₂] (7). Crystals were obtained by electrocrystallization of BET-TTF donor and tetrabutylammonium salt of [Cu(dcdmp)₂][−] as electrolyte, following the same procedure as described for compound 1. Small black needle crystals were collected after 18 days by applying a current density of 1.0 μA·cm^{−2}.

2.3. X-ray Crystallography

X-ray diffraction studies were performed with a Bruker APEX-II CCD detector diffractometer using graphite monochromated Mo-K α radiation ($\lambda = 0.71073 \text{ \AA}$), in the φ and ω scans mode. A semi empirical absorption correction was carried out using SADABS [24]. Data collection, cell refinement, and data reduction were done with the SMART and SAINT programs [25]. X-ray data for the (ET)₂[Ni(dcdmp)₂] compound were collected at room temperature on an Enraf-Nonius CAD-4 (Enraf-nonius, 1989) automatic diffractometer using graphite monochromated Mo-K α ($\lambda = 0.71069 \text{ \AA}$, 50 kV, 26 mA) radiation. Unit-cell dimensions and the orientation matrix were obtained from least-squares refinement of the setting angles of 25 reflections in the range $14^\circ < 2\theta < 24^\circ$. The data set was collected in the ω -2 θ scan mode. The intensities were corrected for Lorentz, polarisation, and absorption effects by empirical corrections based on psi-scans using the Enraf-Nonius reduction program, MoIEN [26]. The structures were solved by direct methods using SIR97 [27] and refined by fullmatrix least-squares methods using the program SHELXL97 [28] using the winGX software package [29]. Non-hydrogen atoms were refined with anisotropic thermal parameters, whereas H-atoms were placed in idealised positions and allowed to refine riding on the parent C atom. Molecular graphics were prepared using Mercury [30]. The positional disorder of S and C atoms in the thiophenic rings (compounds 1, 2T, 3, 4, and 5) was refined by the SHELXL instruction PART (PART 1 and PART 2), and the occupancies of disordered atoms were allowed to refine freely and possess any ratio.

Crystallographic data for α -DT-TTF[Au(dcdmp)₂] (1): C₂₂H₄AuN₈S₁₀, M = 897.90 g·mol⁻¹, monoclinic, space group *P*2₁, *a* = 8.1542(4) Å, *b* = 5.7520(3) Å, *c* = 28.1036(13) Å, β = 96.347(2)°, *V* = 1310.06(11) Å³, *Z* = 2, ρ_{calc} = 2.276 g·cm⁻³, $\mu(\text{Mo } K\alpha)$ = 6.447 mm⁻¹, 9917 reflections measured, 4581 unique [*R*_{int} = 0.0469], θ_{max} = 25.67°, Flack Parameter = 0.06, *R*₁ = 0.0465 using 4338 Refl.>2 σ (*I*), ω *R*₂ = 0.1101, *T* = 150(2) K. CCDC 1826111.

Crystallographic data for BET-TTF[Au(dcdmp)₂] (2M), C₂₂H₈AuN₈S₁₀, M = 901.93 g·mol⁻¹, monoclinic, space group *P*2₁/*c*, *a* = 8.2518(4) Å, *b* = 5.7193(3) Å, *c* = 56.611(3) Å, β = 92.724(3)°, *V* = 2668.7(2) Å³, *Z* = 4, ρ_{calc} = 2.245 g·cm⁻³, $\mu(\text{Mo } K\alpha)$ = 6.330 mm⁻¹, 22517 reflections measured, 4253 unique [*R*_{int} = 0.0508], θ_{max} = 25.02°, *R*₁ = 0.0430 using 3868 Refl.>2 σ (*I*), ω *R*₂ = 0.0809, *T* = 150(2) K. CCDC 1826306; **(2T),** C₂₂H₈AuN₈S₁₀, M = 901.93 g·mol⁻¹, triclinic, space group *P*-1, *a* = 5.7058(3) Å, *b* = 9.6338(5) Å, *c* = 12.8817(6) Å, α = 106.388(2)°, β = 96.438(2)°, γ = 95.743(2)°, *V* = 668.56(6) Å³, *Z* = 1, ρ_{calc} = 2.240 g·cm⁻³, $\mu(\text{Mo } K\alpha)$ = 6.317 mm⁻¹, 5613 reflections measured, 2288 unique [*R*_{int} = 0.0359], θ_{max} = 25.03°, *R*₁ = 0.0260 using 2232 Refl.>2 σ (*I*), ω *R*₂ = 0.0574, *T* = 150(2) K. CCDC 1826112.

Crystallographic data for α -DT-TTF[Cu(dcdmp)₂] (3): C₂₂H₄CuN₈S₁₀, M = 764.47 g·mol⁻¹, monoclinic, space group *P*2₁/*c*, *a* = 15.224(2) Å, *b* = 7.3004(11) Å, *c* = 23.933(2) Å, β = 97.901(5)°, *V* = 2634.7(6) Å³, *Z* = 4, ρ_{calc} = 1.927 g·cm⁻³, $\mu(\text{Mo } K\alpha)$ = 1.657 mm⁻¹, 10849 reflections measured, 4870 unique [*R*_{int} = 0.0976], θ_{max} = 25.68°, *R*₁ = 0.0729 using 2303 Refl.>2 σ (*I*), ω *R*₂ = 0.1426, *T* = 150(2) K. CCDC 1826109.

Crystallographic data for ET[Cu(dcdmp)₂] (4): C₂₂H₈CuN₈S₁₂, M = 832.62 g·mol⁻¹, monoclinic, space group *P*2₁/*c*, *a* = 16.1566(4) Å, *b* = 7.4009(2) Å, *c* = 24.6178(5) Å, β = 100.2440(10)°, *V* = 2896.71(12) Å³, *Z* = 4, ρ_{calc} = 1.909 g·cm⁻³, $\mu(\text{Mo } K\alpha)$ = 1.654 mm⁻¹, 22645 reflections measured, 5475 unique [*R*_{int} = 0.0505], θ_{max} = 25.68°, *R*₁ = 0.0291 using 4591 Refl.>2 σ (*I*), ω *R*₂ = 0.0732, *T* = 150(2) K. CCDC 1826113.

Crystallographic data for (BET-TTF)₂[Cu(dcdmp)₂] (5): C₃₂H₁₆CuN₈S₁₆, M = 1089.03 g·mol⁻¹, triclinic, space group *P*-1, *a* = 8.2678(5) Å, *b* = 8.5858(6) Å, *c* = 14.3566(9) Å, α = 93.248(3)°, β = 92.743(3)°, γ = 108.548(4)°, *V* = 962.29(11) Å³, *Z* = 1, ρ_{calc} = 1.879 g·cm⁻³, $\mu(\text{Mo } K\alpha)$ = 1.478 mm⁻¹, 6512 reflections measured, 3432 unique [*R*_{int} = 0.0371], θ_{max} = 25.35°, *R*₁ = 0.0444 using 2595 Refl.>2 σ (*I*), ω *R*₂ = 0.0956, *T* = 150(2) K. CCDC 1826110.

Crystallographic data for (ET)₂[Ni(dcdmp)₂] (6): C₃₂H₁₆NiN₈S₂₀, M = 1212.42 g·mol⁻¹, triclinic, space group *P*-1, *a* = 7.732(5) Å, *b* = 9.554(5) Å, *c* = 15.254(5) Å, α = 87.990(5)°, β = 89.440(5)°, γ = 72.200(5)°, *V* = 1072.2(10) Å³, *Z* = 1, ρ_{calc} = 1.878 g·cm⁻³, $\mu(\text{Mo } K\alpha)$ = 1.468 mm⁻¹, 4818 reflections measured, 4643 unique [*R*_{int} = 0.0277], θ_{max} = 27.04°, *R*₁ = 0.0589 using 2950 Refl.>2 σ (*I*), ω *R*₂ = 0.0841, *T* = 293(2) K. CCDC 1826114.

Crystallographic data for α -mtdt[Cu(dcdmp)₂] (7): C₂₇H₁₂CuN₁₀S₁₁, M = 892.67 g·mol⁻¹, triclinic, space group *P*-1, *a* = 5.8868(6) Å, *b* = 15.7339(17) Å, *c* = 18.3950(19) Å, α = 83.38°, β = 89.590(4)°, γ = 86.603(5)°, *V* = 1689.4(3) Å³, *Z* = 2, ρ_{calc} = 1.755 g·cm⁻³, $\mu(\text{Mo } K\alpha)$ = 1.367 mm⁻¹, 12286 reflections measured, 5180 unique [*R*_{int} = 0.0834], θ_{max} = 25.68°, *R*₁ = 0.0671 using 2629 Refl.>2 σ (*I*), ω *R*₂ = 0.1370, *T* = 150(2) K. CCDC 1826115.

2.4. Electric Transport Properties

Electrical conductivity measurements were made in single crystals along their long axis using a closed cycle helium refrigerator in the temperature range of 50–320 K and a four-in-line contact configuration by attaching four \varnothing = 25 μ m Au wires to the single crystals with Pt paint (Demetron 308A). The measurement cell [31] is controlled by a computer [32]. In the case of more conducting samples a low-frequency four-probe AC method (77 Hz) was used [33], with a SRS Model SR83 Lock-in Amplifier while applying a 5 μ A current; for the more resistive samples, a four-probe DC method was used instead, using a Keithley 224 current source to apply both direct and reverse DC currents, well below

0.1 μA , through the sample and a Keithley 619 electrometer to measure the corresponding DC voltage. Sample electrodes configuration was checked for un-nested to nested voltage ratio, as defined by Schaffer et al. [34].

3. Results

Electrocrystallization of the donor molecules ET, BET-TTF, α -DT-TTF, and α -mtdt (Scheme 1b) with tetrabutylammonium salts of $[\text{M}(\text{dcdmp})_2]^-$ ($\text{M} = \text{Au}$ (III) and Cu (III)) or $[\text{Ni}(\text{dcdmp})_2]^{2-}$ resulted in crystals of eight new charge transfer salts, α -DT-TTF $[\text{Au}(\text{dcdmp})_2]$ (**1**), BET-TTF $[\text{Au}(\text{dcdmp})_2]$ in two polymorphs (**2M** and **2T**), α -DT-TTF $[\text{Cu}(\text{dcdmp})_2]$ (**3**), ET $[\text{Cu}(\text{dcdmp})_2]$ (**4**), (BET-TTF) $_2[\text{Cu}(\text{dcdmp})_2]$ (**5**), (ET) $_2[\text{Ni}(\text{dcdmp})_2]$ (**6**), and α -mtdt $[\text{Cu}(\text{dcdmp})_2]$ (**7**). These compounds were obtained as single crystals with size and quality suitable for X-ray diffraction and electrical transport properties measurements.

3.1. Single Crystal X-ray Diffraction Analysis

When combining the thiophenic-TTF donors, α -DT-TTF and BET-TTF, with $[\text{Au}(\text{dcdmp})_2]^-$ monoanion, similar crystal structure patterns were obtained, based on mixed donor-acceptor stacks. This pattern had already been observed in the related DT-TTF salts with $[\text{M}(\text{dcdmp})_2]$ ($\text{M} = \text{Au}$, Cu and Ni) [15,16].

α -DT-TTF $[\text{Au}(\text{dcdmp})_2]$ (**1**) crystallizes in the monoclinic system, space group $P2_1$. The asymmetric unit cell contains one $[\text{Au}(\text{dcdmp})_2]^-$ anion and one α -DT-TTF donor molecule, both at general positions (Figure 1a, Table S1). The donor molecule presents a slight boat type distortion, while the $[\text{Au}(\text{dcdmp})_2]^-$ anion is essentially planar, within the range of experimental error (Figure 1a). The donor molecule presents a disorder in the sulphur atom S10 in one of the thiophenic rings with an occupation factor of 59–41% (S10/C21-S10A/C21A).

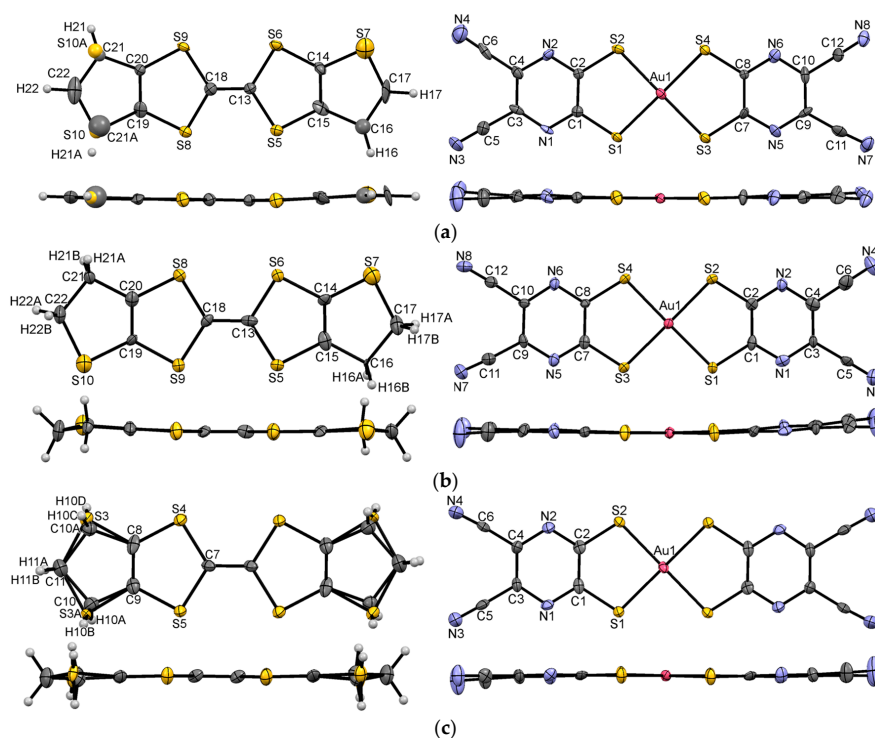


Figure 1. ORTEP and atomic numbering schemes (top and side views) of (a) α -DT-TTF donor molecule and acceptor $[\text{Au}(\text{dcdmp})_2]$ molecule in the crystal structure of **1**; and (b,c) BET-TTF donor molecule and acceptor $[\text{Au}(\text{dcdmp})_2]$ molecule in the crystal structure of **2**: (b) structure M (**2M**) and (c) structure T (**2T**). Thermal ellipsoids drawn at 70% probability level.

The crystal structure of **1** is composed of mixed stacks of alternating donor-acceptor molecules ($D^+A^-D^+A^-D^+A^-$) along the a axis (Figure 2a). Along the stacks there are no short contacts below the sum of van der Waals radii, although the average molecular plane distances between the donor and acceptor molecules of 3.47 Å suggest significant π - π interactions. By contrast, the molecules in neighbouring stacks are connected through a 2D network of short contacts. Along b , the molecules short axis, the stacks are in registry, and several $S\cdots S$ interactions between D^+/D^+ , A^-/A^- and D^+/A^- are observed (Figure 2a₂, Table S2). Along c , the molecules longest axis, the stacks are out-of-registry and D^+/A^- interactions observed are mediated through the nitrile group of the acceptor and the thiophenic sulphur or the hydrogen atoms of the donor molecule (Table S2). Along c , the stacks are related by a 2-fold screw axis, and molecules in nearby stacks have a dihedral angle of $\approx 60^\circ$. This kind of pattern is very similar to those found in the salts family of DT-TTF_m[M(dcdmp)₂]_n (M = Ni, Au and Cu) [15,16].

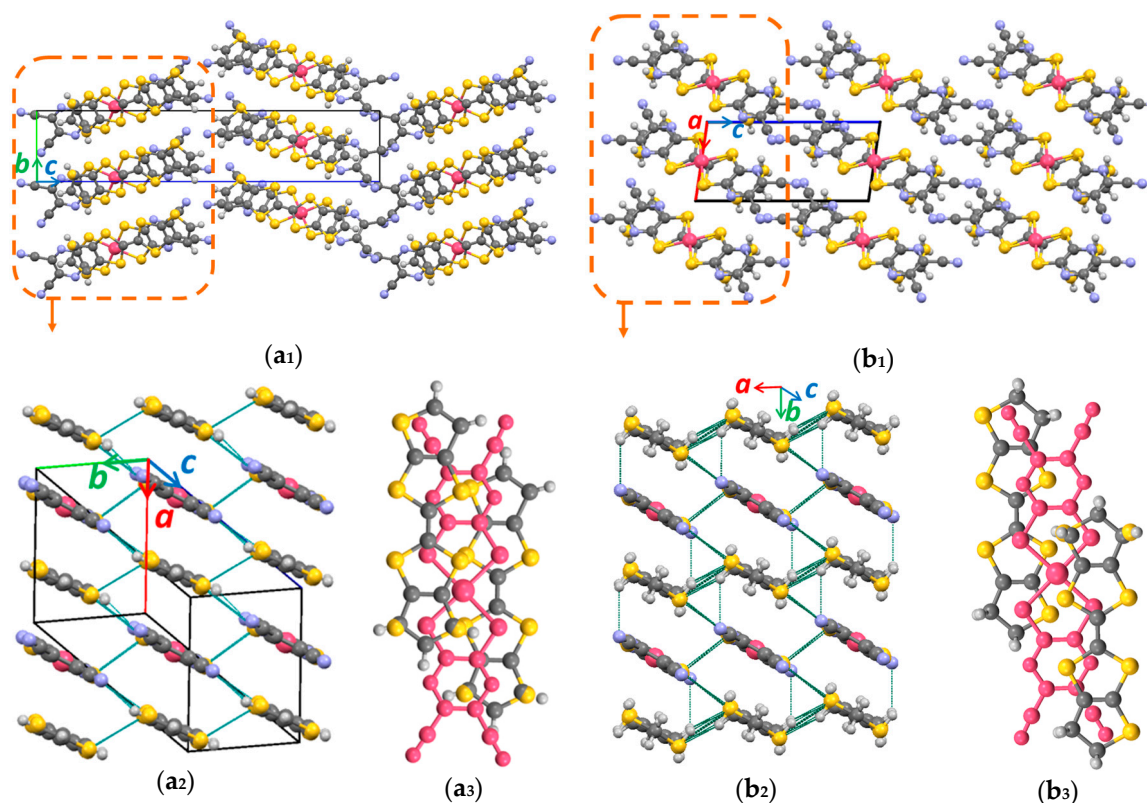


Figure 2. Crystal structure of compound **1** (a) and compound **2T** (b): (a₁,b₁) view along the stacking axis; (a₂,b₂) partial view along the long axis of molecules of neighbouring stacks in the same layer; (a₃,b₃) overlap mode of the mixed stacks. Thin lines represent relevant short contacts.

In the case of BET-TTF[Au(dcdmp)₂] (**2**), two different crystal structures with a 1:1 stoichiometry were obtained from the same preparation by electrocrystallization, with one crystallizing in the monoclinic system space group $P2_1/c$ (**2M**) and the other in the triclinic system space group $P-1$ (**2T**). In both crystal structures, the [Au(dcdmp)₂] acceptor presents bond lengths typical of a monoanion [20,35] and therefore BET-TTF donor molecules must be in a fully oxidized monocationic state.

Although not isostructural, the **2M** salt resembles the crystal structure of **1**. Its asymmetric unit cell contains one independent (BET-TTF)⁺ molecule and one [Au(dcdmp)₂]⁻ anion, with both at general positions (Figure 1b, Table S3). The BET-TTF molecule presents a slight boat type distortion, whilst the [Au(dcdmp)₂] has a very small chair-type distortion (Figure 1b). With a similar packing pattern to **1**, the crystal structure is composed of mixed stacks of alternating donor-acceptor molecules

($D^+A^-D^+A^-D^+A^-$) along the *a* axis (Figure S1). As in **1**, there are no short contacts between molecules along the stacks. Between molecules in neighbouring stacks, the same type of short contacts as in **1** are observed (Table S4).

In the case of **2T**, the unit cell contains one independent BET-TTF⁺ cation and one independent [Au(dcdmp)₂][−] anion, both in an inversion centre (Figure 1c, Table S5). The BET-TTF⁺ molecule is essentially planar, within experimental error, whilst the [Au(dcdmp)₂][−] monoanionic complex presents a slight chair-type distortion (Figure 1c). Unlike in **2M**, in the crystal structure of **2T**, the BET-TTF molecule shows disorder in the thiophenic sulphur atoms S3 with two positions with occupation factors of 79–21% (S3/C10-S3A/C10A). The crystal structure of **2T** is also composed of mixed stacks of alternating donor-acceptor molecules ($D^+A^-D^+A^-D^+A^-$), along the *b* axis (Figure 2b), in the same fashion found in **1** and **2M**. The main difference in **2T** is the relative arrangement between layers, which in this case is “in line” and not related by a dihedral angle of $\approx 60^\circ$ and the displaced overlapping mode between molecules along the stacks (Figure 2a₃,b₃). Polymorph **2T** has a short hydrogen bond (N3⋯H10C–C10A) along the stacks, which is inexistent in the **2M** structure, probably due to the slightly shorter interplanar distances (Figure 2b₂). Apart from these differences, the observed pattern of short contacts between molecules in neighbouring stacks is similar to the observed in compounds **1** and **2M** (Table S6).

In the previously reported salts of [M(dcdmp)₂] with DT-TTF [15], the change of the central transition metal of [M(dcdmp)₂][−] anion, from gold to copper, did not introduce considerable changes in the crystal structure. Nevertheless, in the case of the copper salts an unusual richness of different stoichiometries, 1:1, 2:1, and 3:2 stoichiometries were found, with the crystal structures being arranged both in segregated and mixed stacks of donors and acceptors [15]. α -DT-TTF[Cu(dcdmp)₂] (**3**) was found to be isostructural to the previously reported ET[Au(dcdmp)₂] [35], crystallizing in the monoclinic system, space group *P2*₁/*c*. The asymmetric unit contains one [Cu(dcdmp)₂][−] anion and one donor molecule, both at general positions (Figure 3, Table S7). The donor molecules are planar within experimental error, whereas [Cu(dcdmp)₂][−] anions present a slight boat type distortion (Figure 3). The α -DT-TTF donor molecule in compound **3** presents a disorder in the thiophenic sulphur atoms S7 and S10 over two possible positions with occupation factors of 66–34% (S7/C16-S7A/C16A) and 59–41% (S10/C21-S10A/C21A). The bond length analysis of [Cu(dcdmp)₂][−] confirms its monoanionic state (Table S8), and therefore the donor molecules are fully oxidized.

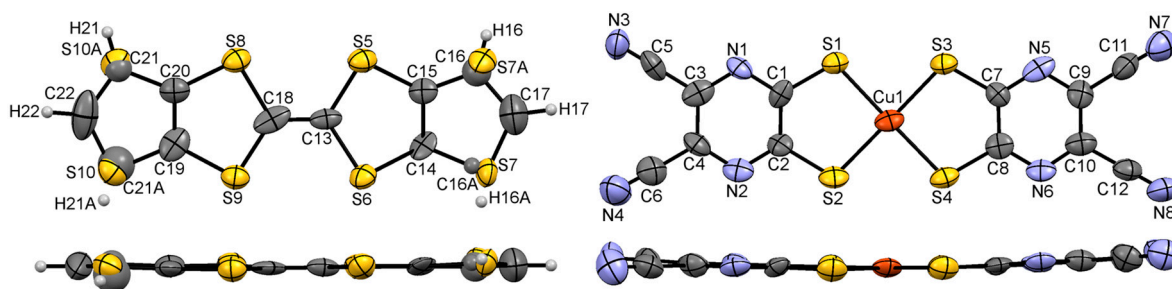


Figure 3. ORTEP and atomic numbering schemes (top and side views) of donor molecules and acceptor [Cu(dcdmp)₂] in the crystal structure of α -DT-TTF[Cu(dcdmp)₂] (**3**), with thermal ellipsoids drawn at 70% probability level.

The crystal structure of **3** shows side-by-side zigzag chains of alternating donor and acceptor molecules ($D^+A^-D^+A^-D^+$), running parallel to the *c* axis (Figure 4), with the acceptor and donor molecules connected through several short S⋯S contacts. Hydrogen bonds, both between the nitrile group or the pyrazine of the anions and the hydrogen atoms in the thiophenic ring of the donor (angle of $\approx 160^\circ$, C16–H16⋯N3 and C21–H21⋯N5), reinforce the short contacts along the chains (Table S9). Along the chain, the average dihedral angles between anions and cations alternate between 4.67° and 54.75° , conferring a wave shape to the chain. Along *b*, the chains are stacked,

forming a 2D network of short S...S contacts between A⁻-D⁺ and D⁺-D⁺ molecules. Apart from the S...S network of short contacts, several hydrogen bonds of the C-H...N and C-H...S type give stability to this 2D structure and also connect acceptor to donor along the *a* axis, parallel to the longest molecular axis of both donor and acceptor molecules (Table S9). The ET[Cu(dcdmp)₂] salt (**4**) is isostructural with **3** (Figures S2 and S3, Tables S8, S10, and S11).

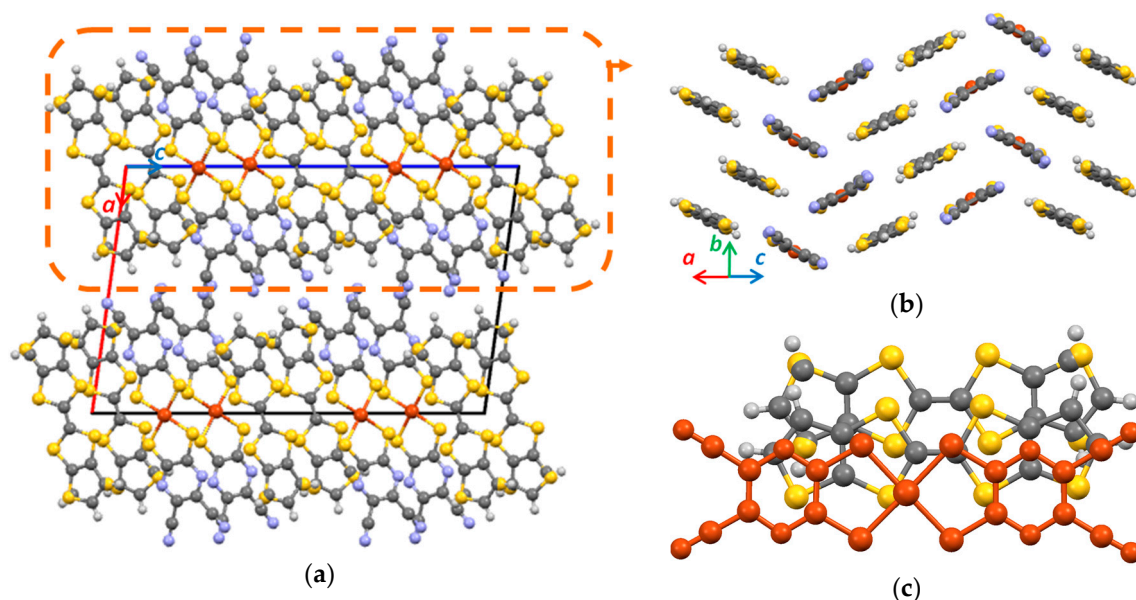


Figure 4. Crystal structure of (α -DT-TTF)[Cu(dcdmp)₂] (**3**): (a) view along the stacking axis; (b) partial view along the long axis of the molecules of neighbouring chains in the same layer; and (c) overlap mode between chains in the same layer.

Another unexpected crystal structure was found when the donor molecule was changed from α -DT-TTF to the relative non-aromatic BET-TTF, which was not isostructural to compound **3** or to compound **2**. In this case, a 2:1 stoichiometry was found, probably due to the spontaneous redox reaction that occurs when combining the [Cu(dcdmp)₂]⁻ monoanion with the donor BET-TTF, leading to a reduction of the acceptor molecule to a dianionic state ($E_{1/2} = +206$ mV) by the full oxidation of the donor molecule ($E_{1/2} = +215$ mV) [18,21].

(BET-TTF)₂[Cu(dcdmp)₂] (**5**) crystallizes in the triclinic system, space group *P*-1. The asymmetric unit is composed of one independent BET-TTF molecule at general position and half [Cu(dcdmp)₂] complex, with the Cu atom in an inversion center (Figure 5a, Table S12), whereas the donor molecule presents a small boat type distortion with the methylene extremities with an envelope type distortion at opposite directions, and the [Cu(dcdmp)₂] anion has a small chair-type distortion (Figure 5a). The BET-TTF donor unit presents disorder in the sulphur atoms of the thiophenic ring over two possible positions, S5 and S8, with occupation factors of 46–54% (in both S5/C10-S5A/C10A and S8/C15-S8A/C15A). The bond lengths analysis indicates that the donor molecule is fully oxidized, while the copper complex is in a dianionic state; therefore, the compound should be formulated as (BET-TTF⁺)₂[Cu(dcdmp)₂]²⁻ (Tables S13 and S14).

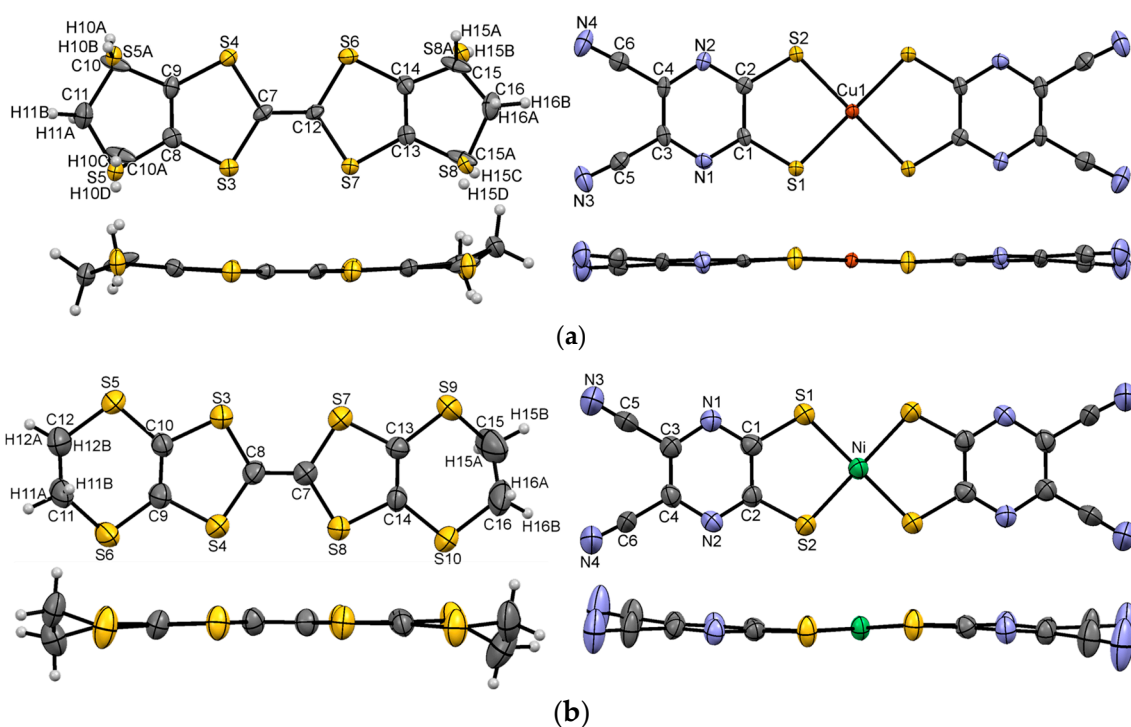


Figure 5. ORTEP and atomic numbering schemes (top and side views) of (a) BET-TTF donor molecule and acceptor $[\text{Cu}(\text{dcdmp})_2]$ in the crystal structure of $(\text{BET-TTF})_2[\text{Cu}(\text{dcdmp})_2]$ (**5**); and (b) ET donor molecules and acceptor $[\text{Ni}(\text{dcdmp})_2]$ in the crystal structure of $(\text{ET})_2[\text{Ni}(\text{dcdmp})_2]$ (**6**), with thermal ellipsoids drawn at 70% probability level.

The crystal structure of **5** is shown in Figure 6a. Its structure is composed of mixed columns along $a+b$ of face-to-face BET-TTF dimers ($(\text{D}^+)_2$) alternating with $[\text{Cu}(\text{dcdmp})_2]^{2-}$ dianions (A^{2-}) with the donor dimers and the dianions placed perpendicularly. The donor molecules in the dimers are connected by four short $\text{S}\cdots\text{S}$ contacts and two $\text{C-H}\cdots\text{S}$ hydrogen bonds ($\text{S3}\cdots\text{S6}$, $\text{S4}\cdots\text{S7}$, and $\text{C15-H15B}\cdots\text{S5}$) with intramolecular distance between average planes of 3.734 Å (Table S15). Along the columns, the acceptor is connected to both molecules of the dimer by short $\text{S}\cdots\text{S}$ and $\text{N}\cdots\text{S}$ contacts (Table S15). Between neighbouring columns, several hydrogen bonds and a short $\text{S}\cdots\text{S}$ contact ($\text{C16-H16A}\cdots\text{N2}$, $\text{C11-H11B}\cdots\text{N3}$, and $\text{S1}\cdots\text{S3}$) connect acceptor and donor dimers. Between the extremities of the molecules, the stacks are also connected, along c , by a hydrogen bond between acceptor and donor and a short $\text{N3}\cdots\text{N3}$ contact between acceptors. Apart from the strong dimer interaction, there are no contacts between different donor dimers in neighbouring columns.

$(\text{ET})_2[\text{Ni}(\text{dcdmp})_2]$ (**6**) was also found to have a 2:1 stoichiometry. Compound **6** crystallizes in the triclinic system, space group $P-1$. The asymmetric unit cell contains an independent $[\text{Ni}(\text{dcdmp})_2]^{2-}$ located at an inversion centre and one ET^+ molecule at general position (Figure 5b, Table S16). The average bond length M-S value (2.175 Å), found in the acceptor, indicates that the complex is in a dianionic state [36]. The nickel dianion presents a slight chair type distortion, and the ET molecule shows the usual geometry found in other related salts of this donor (Figure 5b) [37]. In spite of the uniform color and shape of the crystals obtained in one preparation, the presence of other stoichiometries or phases cannot be excluded, since EPR measurements in crystals from the same preparation present two different shapes (Figures S4 and S5). Attempts to prepare other $[\text{Ni}(\text{dcdmp})_2]$ salts with BET-TTF, α -DT-TTF, or α -mtdt using electrocrystallization techniques did not yield good quality single crystals for X-ray diffraction and electric transport properties measurements.

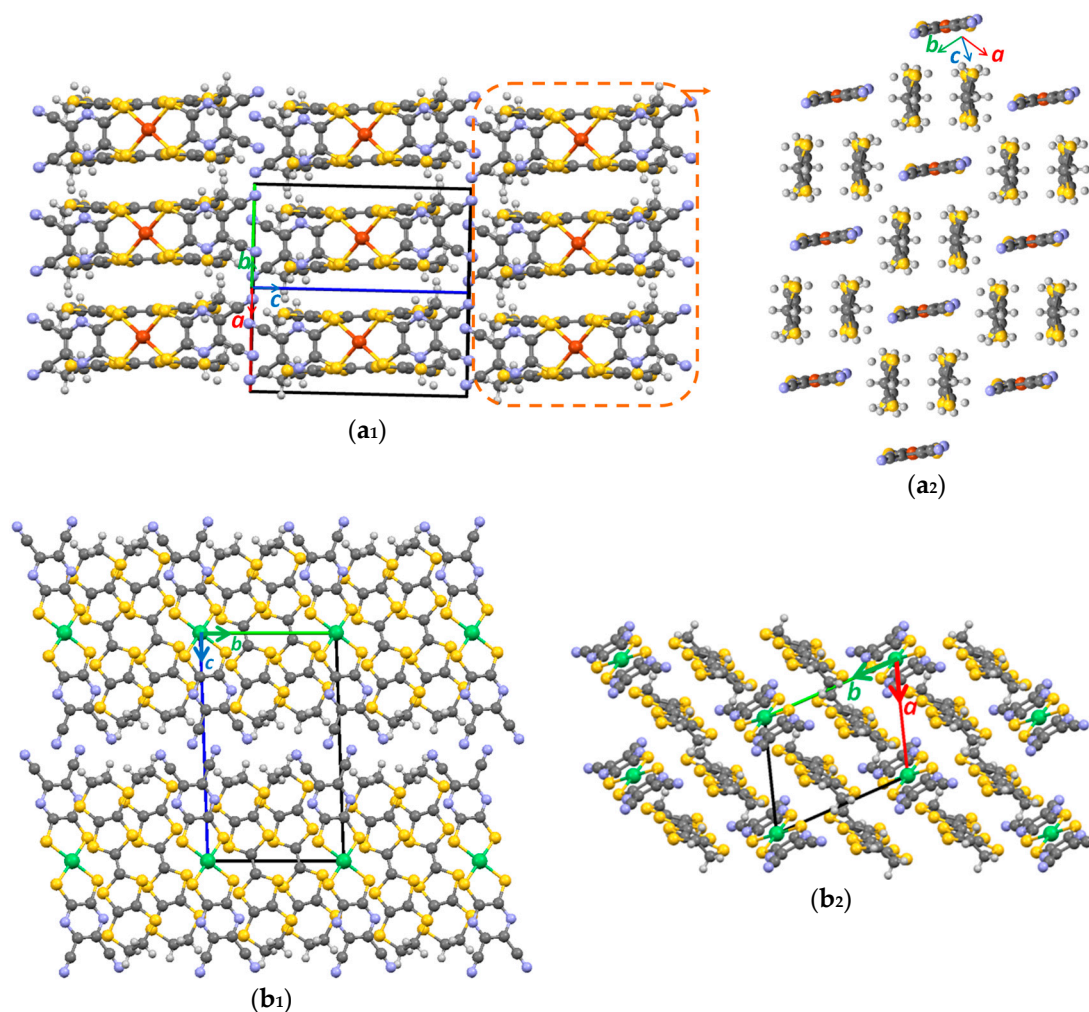


Figure 6. Crystal structure of compound 5 (a) and compound 6 (b): (a₁) view along *a*-*b*; (a₂) partial view along the long axis of the molecules of neighbouring columns in the same layer, with the alternating dianions and BET-TTF dimers; (b₁) view along the stacking axis; (b₂) partial view of the layers in the *ab* plane.

Similarly to $\text{ET}[\text{Cu}(\text{dcdmp})_2]$ (4) and $\alpha\text{-DT-TTF}[\text{Cu}(\text{dcdmp})_2]$ (3), the crystal structure of $(\text{ET})_2[\text{Ni}(\text{dcdmp})_2]$ (6) is composed of layers of zigzag chains, along the *b* axis, of dianions alternating with donor dimers $(\text{A}^{2-})\text{D}^+\text{D}^+(\text{A}^{2-})\text{D}^+\text{D}^+(\text{A}^{2-})$ (Figure 6b). Along a chain there are several $\text{S}\cdots\text{S}$ and $\text{S}\cdots\text{N}$ short contacts both between donors and acceptor-donor molecules (Table S17). In the *ab* plane, these chains interact with each other through short $\text{Ni}\cdots\text{S}$ contacts between acceptor-donor molecules and several $\text{C-H}\cdots\text{S}$ hydrogen bonds between donors ($\text{C12-H12B}\cdots\text{S9-}$, $\text{C11-H11B}\cdots\text{S9}$, $\text{C16-H16A}\cdots\text{S5}$). Along *c*, the contact between chains is made by acceptor-donor hydrogen bonds ($\text{C16-H16B}\cdots\text{N3}$). Another way to describe this structure is to see it as composed layers, in the *ab* plane, as a bidimensional layer of pairs of ET molecules coupled face-by-face that are connected with other pairs by a short, side-by-side, $\text{S}\cdots\text{S}$ contacts. In the “channels” of the layers are located the acceptors surrounded by donors in all directions. There are no interactions between acceptors.

With $\alpha\text{-mtdt}$, a dissymmetric TTF-type donor, only the copper salt could be isolated. $\alpha\text{-mtdt}[\text{Cu}(\text{dcdmp})_2]$ (7) crystallizes in the triclinic system, space group *P*-1. The asymmetric unit contains one independent $(\alpha\text{-mtdt})^+$ molecule at general position and two $[\text{Cu}(\text{dcdmp})_2]^-$ complexes, both with the Cu atom in an inversion centre (Figure 7, Tables S18 and S19). The $\alpha\text{-mtdt}$ molecule is essentially planar, with the exception of the $-(\text{CH}_2)_2\text{-CN}$ groups that point out both in the same

direction almost perpendicularly to the central molecular plane, while both $[\text{Cu}(\text{dcdmp})_2]$ molecules present a very small chair-type distortion (Figure 7). The bond length analysis confirms that the donor molecule is fully oxidized $(\alpha\text{-mtdt})^+$ (Table S20) and the copper dithiolene complex is in monoanionic state (Table S21).

Figure 8a,b illustrates the crystal structure of compound 7, which are composed of segregated stacks of donors and acceptors, along the a axis, with sheets of stacks of $\alpha\text{-mtdt}$ donors and $[\text{Cu}(\text{dcdmp})_2]$ acceptors alternating along b . Within the stacks, the donor molecules are arranged in a head-to-head fashion with distance of 3.469 Å between molecular planes, suggesting significant $\pi\text{-}\pi$ interactions. The overlap mode of $\alpha\text{-mtdt}$ donors (Figure 8c) shows a large displacement of the molecules along their long axis, probably due to the bulky cyanoethyl group. Within the stacks, the donor molecules are connected by two short S \cdots S contacts (S5 \cdots S11 and S6 \cdots S10). The two acceptor molecules A and B (respectively, red and blue molecules in Figure 8a,b), although crystallographically distinct, are identical within experimental uncertainty and present identical overlap modes (Figure 8d). Along each monoanion stack, A or B, there are no short contacts, and the distance between molecular planes is of 3.516 Å and 3.501 Å, respectively. Short contacts between acceptor molecules A and B are also inexistent. The different acceptor stacks have different angles in relation to the $\alpha\text{-mtdt}$ donor stacks, with a dihedral angle of 37.47° and 74.14° for stacks of molecules A and B, respectively. The interactions between stacks are made in two distinct ways along the $\alpha\text{-mtdt}$ molecule long axis (Table S22): (a) on one side, the donor molecules interact with each other through C–H \cdots N hydrogen bonds (C22–H22B \cdots N10 and C23–H23B \cdots N9, Figure S6) and also with the acceptor stacks of molecule A (red molecule in Figure 8a,b) through C–H \cdots S hydrogen bonds (C25–H25A \cdots N4, Figure S7); (b) on the other side, the interaction is between the methyl groups and the thiophenic sulphur atom of the $\alpha\text{-mtdt}$ donor through a hydrogen bond (Figure S6, C18–H18A \cdots S7). The lateral connection between acceptor-donor molecules along the molecules minor axis is mediated by short S \cdots S and S \cdots N contacts and hydrogen bonds interactions (Table S22, Figure S7).

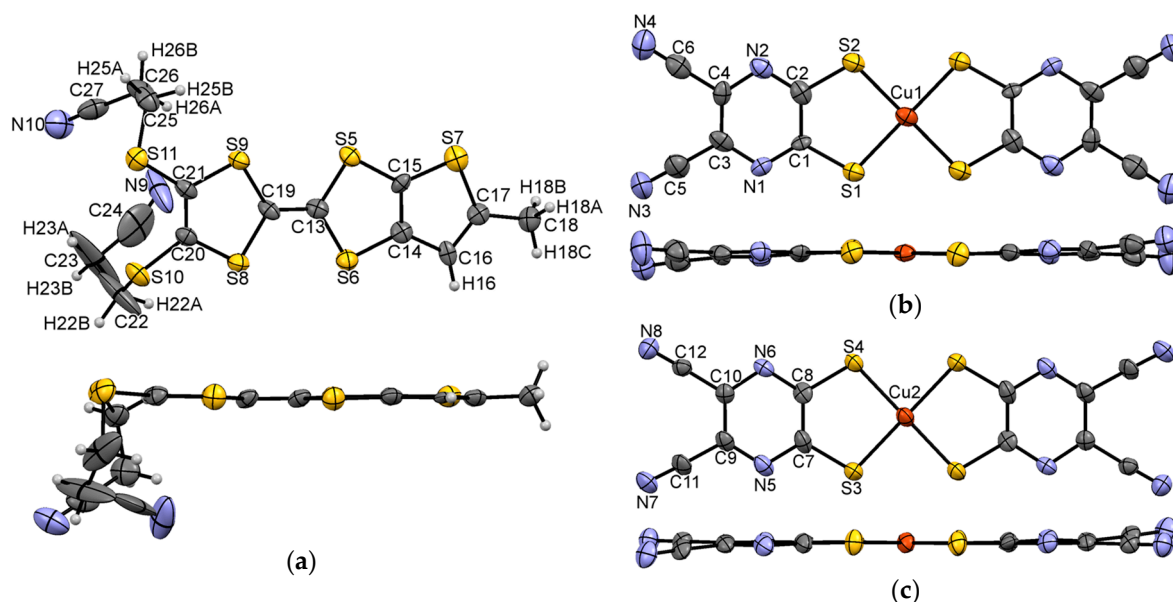


Figure 7. ORTEP and atomic numbering schemes (top and side views) of $\alpha\text{-mtdt}$ donor (a) and acceptor $[\text{Cu}(\text{dcdmp})_2]$ molecules A (b) and B (c) in the crystal structure of $(\alpha\text{-mtdt})[\text{Cu}(\text{dcdmp})_2]$ (7), with thermal ellipsoids drawn at 50% probability level.

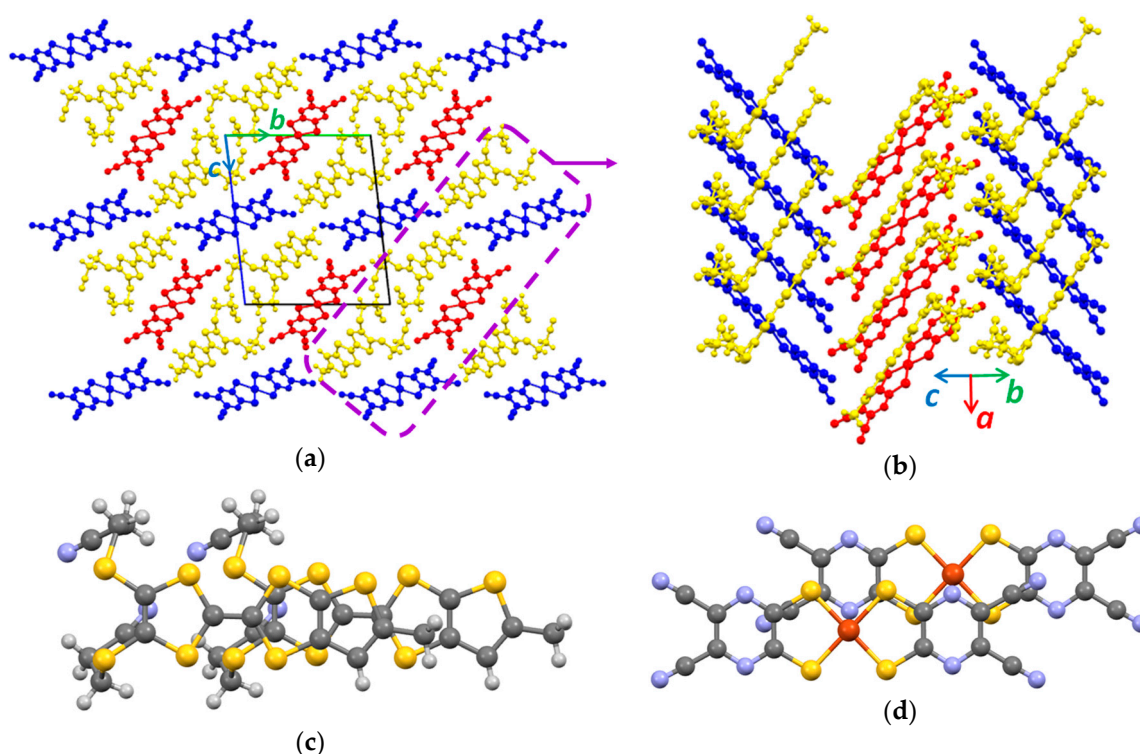


Figure 8. Crystal structure of $(\alpha\text{-mtdt})[\text{Cu}(\text{dcdmp})_2]$ (7): (a) view along the *a* axis; (b) partial view showing the different segregated stacks of donors (yellow) and acceptor stacks (red and blue) and overlap mode representation between donors (c) and between acceptor stacks (d).

3.2. Electric Transport Properties

The electrical conductivity of compounds 1–7 was measured in single crystals along their long axis, and the results are presented in Figure 9 and Table 1. All compounds present a semiconducting behaviour with room temperature values in the range $\approx 10^{-5} \text{ S/cm} < \sigma_{\text{RT}} < \approx 10^{-1} \text{ S/cm}$. The highest conductivity was found for the 1:1 copper compound 3 and gold salt 1 of $\alpha\text{-DT-TTF}$ donor, followed closely by $(\text{BET-TTF})[\text{Au}(\text{dcdmp})_2]$ (2). The modest conductivity values and the thermally activated behaviour observed were not unexpected in view of the fully oxidised nature of the donor molecules, which are expected to lead to Mott insulator states. In this sense, the relatively large conductivity values observed in $\alpha\text{-DT-TTF}$ salts 1 and 3 are very large for 1:1 salts with fully oxidised molecules. In $(\alpha\text{-DT-TTF})[\text{Au}(\text{dcdmp})_2]$ (1), resistivity measurements made in needle (0.16 S/cm) and plate shaped sample (0.052 S/cm), which were obtained in the same preparation, gave slightly different values, which could indicate the possibility of different phases. The coexistence of different stoichiometries and polymorphs is not unprecedented in salts with the $[\text{M}(\text{dcdmp})_2]$ anions [15]. However, this possibility could not be confirmed from the different crystals selected for single crystal X-ray diffraction.

It should be noted that in compounds 1, 2, and 3 with higher conductivity, both the donor and acceptor molecules make an extended network of interactions, and both could provide conduction bands. In compound 7, the bulkier cyanoethyl groups of the asymmetric donor molecule $\alpha\text{-mtdt}$ act as a hindrance to the donor molecules overlapping each other; nevertheless, a crystal structure pattern based on segregated stacks of donor and acceptors was obtained with a room temperature conductivity of $1.1 \times 10^{-3} \text{ S/cm}$.

Although $\text{ET}[\text{Cu}(\text{dcdmp})_2]$ (4) is isostructural with 3, it presents one of the lowest conductivities found in this group of compounds ($4.2 \times 10^{-4} \text{ S/cm}$). Even though compound 4 seems to have a good overlap with the donor molecules along the *b* axis (Figure 4c and Figure S3), a detailed crystal structure

analysis shows that the distances between the molecular average planes might prevent effective π - π interactions, with donor interplanar distances larger in compound **4** than in **3** (3.699 Å and 3.357 Å for compound **4** and 3.571 Å and 3.033 Å in compound **3**).

The room temperature conductivities of compounds **5** and **6**, both in a 2:1 stoichiometry, are of the same order of magnitude as that found in **4**. The dimeric nature of the donors found in these crystal structures probably induces electron localization and, even with a network of interactions between donors, effective electronic pathways are not established.

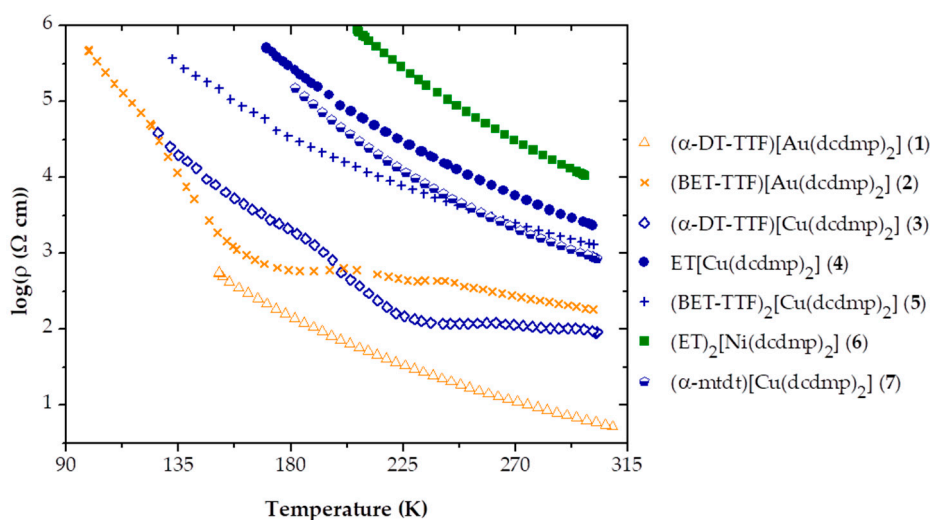


Figure 9. Electrical resistivity ρ of compounds 1–7 as a function of temperature T .

Table 1. Room-temperature electrical conductivity (σ_{RT}) and activation energy (E_a) of compounds 1–7.

CT Salts	σ_{RT} (S/cm)	E_a (meV)
(ET) ₂ [Ni(dcdmp) ₂] (6)	9.4×10^{-5}	128
(ET)[Cu(dcdmp) ₂] (4)	4.2×10^{-4}	190
(BET-TTF) ₂ [Cu(dcdmp) ₂] (5)	7.4×10^{-4}	134
(α -mtdt)[Cu(dcdmp) ₂] (7)	1.1×10^{-3}	207
(BET-TTF)[Au(dcdmp) ₂] (2)	5.4×10^{-3}	95
(α -DT-TTF)[Au(dcdmp) ₂] (1)	5.2×10^{-2} ^a ; 1.6×10^{-1} ^b	105 ^a ; 59 ^b
(α -DT-TTF)[Cu(dcdmp) ₂] (3)	1.1×10^{-2}	107

^a Plate; ^b Needle.

4. Conclusions

Eight new compounds were obtained by electrocrystallization by combining TTF type electronic donors, namely, ET, BET-TTF, α -DT-TTF, and α -mtdt, with transition metal complexes [M(dcdmp)₂] (M = Au, Cu, and Ni). Most of the herein reported compounds present a 1:1 stoichiometry with a crystal structure composed of mixed stacks of donor and acceptor molecules, with the exception of (α -mtdt)[Cu(dcdmp)₂] (**7**), which crystallizes in segregated stacks of donors and acceptors. Other two exceptions are the salts (BET-TTF)₂[Cu(dcdmp)₂] (**5**) and (ET)₂[Ni(dcdmp)₂] (**6**) that present a 2:1 stoichiometry. All compounds showed a semiconducting behavior with a room conductivity ranging from 1.6×10^{-1} to 9.4×10^{-5} S/cm. The highest room temperature conductivity was observed for (α -DT-TTF)[Au(dcdmp)₂] (**1**) and the lowest for (ET)₂[Ni(dcdmp)₂] (**6**).

The pyrazine nitrogen atoms in the dcdmp ligand were found, amongst the different crystal structures, to be extensively involved in both S \cdots N short contacts and N \cdots H–C hydrogen bonds. As a consequence, when comparing the salts of the complexes based on dcdmp ligands with the mnt

ligand, the structures are quite different. The diversity of crystal structures and polymorphs in this family of compounds makes them good models for further understanding the correlation between the intermolecular crystal structure patterns and the observed macroscopic electrical transport properties.

Supplementary Materials: CCDC 1826109-1826115 and 1826306 contains the supplementary crystallographic data for this paper. These data can be obtained free of charge via <http://www.ccdc.cam.ac.uk/conts/retrieving.html>. The following are available online at www.mdpi.com/xxx/s1, Table S1: Bond lengths of compound 1, Table S2: short contacts of compound 1. Table S3: bond lengths of compound 2M, Figure S1: crystal structure of compound 2M, Table S4: short contacts of compound 2M, Table S5: bond lengths of compound 2T, Table S6: short contacts of compound 2T, Table S7: bond lengths of compound 3, Table S8: acceptor molecule bond length analysis of compound 3 and 4, Table S9: short contacts of compound 3, Figure S2: ORTEP of compound 4, Figure S3: crystal structure of compound 4, Table S10: bond lengths of compound 4, Table S11: short contacts of compound 4, Table S12: bond lengths of compound 5, Tables S13 and S14: bond length analysis of compound 5, Table S15: short contacts of compound 5, Table S16: bond lengths of compound 6, Table S17: short contacts of compound 6, Figures S4 and S5: EPR measurements of compound 6, Tables S18 and S19: bond lengths of compound 7, Tables S20 and S21: bond length analysis of compound 7, Table S22: short contacts of compound 7, Figures S6 and S7: relevant short contacts of compound 7.

Acknowledgments: This work was supported by FCT (Portugal) through contracts PTDC/QEQ-SUP/1413/2012 and UID/Multi/04349/2013 and FCTs grants of R.A.L.S (SFRH/BD/86131/2012) and S.R. (SFRH/BPD/113344/2015).

Author Contributions: Dulce Belo, Vasco Gama, and Manuel Almeida conceived and designed the experiments; Rafaela A. L. Silva performed the experiments; Isabel C. Santos analyzed the crystallographic data; Sandra Rabaça analyzed the cyclic voltammetry; Elsa B. Lopes measured the electric transport properties and Rafaela A. L. Silva, Dulce Belo, and Manuel Almeida wrote the paper with contributions from all authors.

Conflicts of Interest: The authors declare no conflict of interest. The founding sponsors had no role in the design of the study; in the collection, analyses, or interpretation of data; in the writing of the manuscript; or in the decision to publish the results.

References

1. Kato, R. Conducting Metal Dithiolene Complexes: Structural and Electronic Properties. *Chem. Rev.* **2004**, *104*, 5319–5346. [[CrossRef](#)] [[PubMed](#)]
2. Stiefel, E.I. *Dithiolene Chemistry. Synthesis, Properties and Applications*; John Wiley & Sons, Inc.: Hoboken, NJ, USA, 2004.
3. Coomber, A.T.; Beljonne, D.; Friend, R.H.; Brédas, J.L.; Charlton, A.; Robertson, N.; Underbill, A.E.; Kurmoo, M.; Day, P. Intermolecular interactions in the molecular ferromagnetic $\text{NH}_4\text{Ni}(\text{mnt})_2 \cdot \text{H}_2\text{O}$. *Nature* **1996**, *380*, 144–146. [[CrossRef](#)]
4. Fourmigué, M.; Domercq, B.; Jourdain, I.V.; Molinié, P.; Guyon, F. Amaudrut, Interplay of Structural Flexibility and Crystal Packing in a Series of Paramagnetic Cyclopentadienyl/Dithiolene Mo and W Complexes: Evidence for Molecular Spin Ladders. *Chem. A Eur. J.* **1998**, *4*, 1714–1723. [[CrossRef](#)]
5. Rovira, C. Molecular Compounds Showing a Spin Ladder Behaviour. In *π -Electron Magnetism from Molecules to Magnetic Materials*; Veciana, J., Ed.; Springer: Berlin/Heidelberg, Germany, 2001; Volume 100, pp. 163–188.
6. Underhill, A.E.; Ahmad, M.M. A new one-dimensional ‘metal’ with conduction through bis(dicyanoethylenedithiolato) platinum anions. *J. Chem. Soc. Chem. Commun.* **1981**, 67–68. [[CrossRef](#)]
7. Ahmad, M.M.; Turner, D.J.; Underhill, A.E.; Jacobsen, C.S.; Mortensen, K.; Carneiro, K. Physical properties and the Peierls instability of $\text{Li}_{0.82}[\text{Pt}(\text{S}_2\text{C}_2(\text{CN})_2)_2] \cdot 2\text{H}_2\text{O}$. *Phys. Rev. B* **1984**, *29*, 4796–4799. [[CrossRef](#)]
8. Brossard, L.; Ribault, M.; Bousseau, M.; Valade, L.; Cassoux, P. Un nouveau type de supraconducteur moléculaire: $\text{TTF}[\text{Ni}(\text{dmit})_2]_2$. *Comptes Rendus Acad. Sci.* **1986**, *302*, 205–210.
9. Cassoux, P. Molecular (super)conductors derived from bis-dithiolate metal complexes. *Coord. Chem. Rev.* **1999**, *185–186*, 213–232. [[CrossRef](#)]
10. Robertson, N.; Cronin, L. Metal bis-1,2-dithiolene complexes in conducting or magnetic crystalline assemblies. *Coord. Chem. Rev.* **2002**, *227*, 93–127. [[CrossRef](#)]
11. Rabaça, S.; Almeida, M. Dithiolene complexes containing N coordinating groups and corresponding tetrathiafulvalene donors. *Coord. Chem. Rev.* **2010**, *254*, 1493–1508. [[CrossRef](#)]
12. Ribas, X.; Dias, J.C.; Morgado, J.; Wurst, K.; Almeida, M.; Veciana, J.; Rovira, C. Novel Cu(III) bis-1,2-diselenolene complex with a highly extended 3D framework through Na^+ coordination. *CrystEngComm* **2002**, *4*, 564–567. [[CrossRef](#)]

13. Ribas, X.; Dias, J.C.; Morgado, J.; Wurst, K.; Santos, I.C.; Almeida, M.; Vidal-Gancedo, J.; Veciana, J.; Rovira, C. Alkaline Side-Coordination Strategy for the Design of Nickel(II) and Nickel(III) Bis(1,2-diselenolene) Complex Based Materials. *Inorg. Chem.* **2004**, *43*, 3631–3641. [[CrossRef](#)] [[PubMed](#)]
14. Ribas, X.; Dias, J.C.; Morgado, J.; Wurst, K.; Molins, E.; Ruiz, E.; Almeida, M.; Veciana, J.; Rovira, C. Novel Cu^{III} bis-1,2-dichalcogenene complexes with tunable 3D framework through alkaline cation coordination. A structural and theoretical study. *Chem. Eur. J.* **2004**, *10*, 1691–1704. [[CrossRef](#)] [[PubMed](#)]
15. Silva, R.A.L.; Santos, I.C.; Lopes, E.B.; Rabaça, S.; Gancedo, V.-J.; Rovira, C.; Almeida, M.; Belo, D. DT–TTF Salts with [Cu(dcdmp)₂][−]: The Richness of Different Stoichiometries. *Cryst. Growth Des.* **2016**, *16*, 3924–3931. [[CrossRef](#)]
16. Belo, D.; Lopes, E.B.; Santos, I.C.; Dias, J.C.; Figueira, M.; Almeida, M.; Fourmigué, M.; Rovira, C. Synthesis and Characterization of Charge Transfer Salts. *J. Low Temp. Phys.* **2006**, *142*, 349–354. [[CrossRef](#)]
17. Rovira, C.; Veciana, J.; Santalo, N.; Tarres, J.; Cirujeda, J.; Molins, E.; Llorca, J.; EspinoSa, E. Synthesis of Several Isomeric Tetrathiafulvalene. π -Electron Donors with Peripheral Sulfur Atoms. A Study of Their Radical Cations. *J. Org. Chem.* **1994**, *59*, 3307–3313.
18. Silva, R.A.L.; Neves, A.I.; Afonso, M.L.; Santos, I.C.; Lopes, E.B.; Del Pozo, F.; Pfattner, R.; Torrent, M.M.; Rovira, C.; Almeida, M.; et al. α -Dithiophene-tetrathiafulvalene—A Detailed Study of an Electronic Donor and Its Derivatives. *Eur. J. Inorg. Chem.* **2013**, *13*, 2440–2446. [[CrossRef](#)]
19. Silva, R.A.L.; Vieira, B.J.C.; Andrade, M.A.; Santos, I.C.; Rabaça, S.; Belo, D.; Almeida, M. TTFs nonsymmetrically fused with alkylthiophenic moieties. *Beilstein J. Org. Chem.* **2015**, *11*, 628–637. [[CrossRef](#)] [[PubMed](#)]
20. Belo, D.; Santos, I.C.; Almeida, M. 5,6-Dicyano-2,3-dithiopyrazine (dcdmp) chemistry: Synthesis and crystal structure of Au(III)(dcdmp)₂ complexes and 2,3,7,8-tetracyano-1,4,6,9-tetraazothianthrene. *Polyhedron* **2004**, *23*, 1351–1359. [[CrossRef](#)]
21. Belo, D.; Figueira, M.J.; Santos, I.C.; Gama, V.; Pereira, L.C.; Henriques, R.T.; Almeida, M. Synthesis and characterization of copper complexes with the 2,3-dicyano-5,6-dimercaptopyrazine ligand: Magnetic properties of a ferrocenium salt. *Polyhedron* **2005**, *24*, 2035–2042. [[CrossRef](#)]
22. Tomura, M.; Tanaka, S.; Yamashita, Y. Synthesis, structure and properties of the novel conductingdithiolato-metal complexes having dicyanopyrazine moieties. *Synth. Met.* **1994**, *64*, 197–202. [[CrossRef](#)]
23. Perrin, D.D.; Armarego, W.L.F. *Purification of Laboratory Chemicals*, 3rd ed.; Pergamon Press: Oxford, UK, 1988.
24. Sheldrick, G.M. *SADABS*; Bruker AXS Inc.: Madison, WI, USA, 2004.
25. Bruker. *SMART and SAINT*; Bruker AXS Inc.: Madison, WI, USA, 2008.
26. Fair, C.K. *MoIEN. An Interactive Intelligent System for Crystal Structure Analysis*; Enraf-Nonius: Delft, The Netherlands, 1990.
27. Altomare, A.; Burla, M.C.; Camalli, M.; Cascarano, G.; Giacovazzo, G.; Guagliardi, A.; Moliterni, A.G.G.; Polidori, G.; Spagna, R. *SIR97: A new tool for crystal structure determination and refinement*. *J. Appl. Cryst.* **1999**, *32*, 115–119. [[CrossRef](#)]
28. Sheldrick, G.M. A short history of SHELX. *Acta Crystallogr. A Found. Crystallogr.* **2008**, *64*, 112–122. [[CrossRef](#)] [[PubMed](#)]
29. Farrugia, L.J. WinGX and ORTEP for Windows: An update. *J. Appl. Cryst.* **2012**, *45*, 849–854. [[CrossRef](#)]
30. Macrae, C.F.; Bruno, I.J.; Chisholm, J.A.; Edgington, P.R.; McCabe, P.; Pidcock, E.; Rodriguez-Monge, L.; Taylor, R.; van de Streek, J.; Wood, P.A. Mercury CSD 2.0—New features for the visualization and investigation of crystal structures. *J. Appl. Cryst.* **2008**, *41*, 466–470.
31. Almeida, M.; Alcácer, L.; Oostra, S. Anisotropy of thermopower in *N*-methyl-*N*-ethylmorpholinium bistetracyanoquinodimethane, MEM(TCNQ)₂, in the region of the high-temperature phase transitions. *Phys. Rev. B* **1984**, *30*, 2839–2844. [[CrossRef](#)]
32. Lopes, E.B. *Internal Report*; INETI-Sacavém: Lisbon, Portugal, 1991.
33. Chaikin, P.M.; Kwak, J.F. Apparatus for Thermopower Measurements on Organic Conductors. *Rev. Sci. Instrum.* **1975**, *46*, 218–220. [[CrossRef](#)]
34. Schaffer, P.E.; Wudl, F.; Thomas, G.A.; Ferraris, J.P.; Cowan, D.O. Apparent giant conductivity peaks in an anisotropic medium: TTF-TCNQ. *Solid State Commun.* **1974**, *14*, 347–351. [[CrossRef](#)]

35. Belo, D.; Morgado, J.; Lopes, E.B.; Santos, I.C.; Rabaça, S.; Duarte, M.T.; Gama, V.; Henriques, R.T.; Almeida, M. Synthesis and Characterisation of Charge Transfer Salts Based on Au(dcdmp), and TTF Type Donors. *Synth. Met.* **1999**, *102*, 1751–1752. [[CrossRef](#)]
36. Tomura, M. Bis(tetra-n-butylammonium) bis(5,6-dicyanopyrazine-2,3-dithiolato- κ 2S,S')nickelate(II). *IUCrData* **2017**, *2*, x171059. [[CrossRef](#)]
37. Kobayashi, H.; Kobayashi, A.; Sasaki, Y.; Saito, G.; Inokuchi, H. The Crystal and Molecular Structures of Bis(ethylenedithio)tetrathiafulvalene. *Bull. Chem. Soc. Jpn.* **1986**, *59*, 301–302. [[CrossRef](#)]



© 2018 by the authors. Licensee MDPI, Basel, Switzerland. This article is an open access article distributed under the terms and conditions of the Creative Commons Attribution (CC BY) license (<http://creativecommons.org/licenses/by/4.0/>).